EFFECTS OF MILLING TIME ON MORPHOLOGY AND ELECTROCHEMICAL PERFORMANCE OF $Li_4Ti_5O_{12}$/C COMPOSITE ANODE

M. I. Ishak, A. Mokhtar, M. A. Sulaiman, A. Mat, K. S Sulaiman,
M. F. Rosle and S. M. Hasanaly

Energy Materials Section, Advanced Materials Research Centre (AMREC),
SIRIM Berhad, Lot 34, Jalan Hi-Tech 2/3, Kulim Hi-Tech Park,
09000 Kulim, Kedah, MALAYSIA.

ABSTRACT

The $Li_4Ti_5O_{12}$/C anode material was prepared via high energy ball milling method for 2, 4, 6 and 8 hours and subsequently heat treated at 850° C for 12 hours in N_2 atmosphere. The structure and morphology of the prepared $Li_4Ti_5O_{12}$/C composite was characterized by means of X-Ray Diffractometry (XRD) and Field-Emission Scanning Electron Microscope (FESEM). The morphological changes of the $Li_4Ti_5O_{12}$/C composite resulted from different milling time strongly influences the electrochemical performance of this anode material. The $Li_4Ti_5O_{12}$/C composite which was milled for 2 hours delivered the best electrochemical performance with a discharge capacity of 154 $mAhg^{-1}$ when cycled between 1.0 and 3.0 V vs. Li/Li$^+$. Particulate morphology observed from FESEM images showed that samples that were milled for 8 hours have increased agglomeration compared to that milled for 2, 4 and 6 hours. The larger surface area for reaction with Li$^+$ improves the discharge capacity of the $Li_4Ti_5O_{12}$/C anode material.

Keywords: $Li_4Ti_5O_{12}$/C; high energy ball milling; morphology; anode

INTRODUCTION

The increasing demand for electric vehicles (EV) presents a challenge to identify battery with low-cost materials with high power performance. A key element in batteries powering EV is high power capability [1]. Most electronic devices battery uses graphite as the anode material. The carbonaceous based anode can provide battery with high specific capacity at higher working voltage. However, this material is not suitable for high power drain applications which need longer cycle life such as hybrid and electric vehicle. Lithium titanate oxide was introduced by Ohzuku et al [2] as an alternative anode material has a 'zero strain' structure. This material exhibits excellent life cycle which is must suitable for automotive application. Despite these advantages, $Li_4Ti_5O_{12}$ still suffers from problems of poor high-rate performance arising from its low electrical conductivity (10^{-13} Scm^{-1}). To overcome this problem, considerable efforts have been made and one of the most promising strategies is to fabricate nanostructured $Li_4Ti_5O_{12}$ [3-10]. By reducing the particle dimensions to nanoscale, the distance of electron and lithium-ion transport is shortened and the contact area between electrode and electrolyte is increased, which will lead to the improved electrochemical

performance [3-10]. The lack of appreciable electronic conductivity can be compensated by carbon coating such as polyethylene glycol (PEG) and other sources of carbon. In this work, $Li_4Ti_5O_{12}$/C was prepared by a ball milling assisted solid state process. This technique does not involve complicated process and practical to use for mass production and lower cost. This paper will discuss on the effect of structure, morphology and electrochemical performance of the synthesized $Li_4Ti_5O_{12}$/C as an anode material based on different milling time

EXPERIMENTAL

The starting materials, TiO_2-anatase (Aldrich, USA) and Li_2CO_3 (Aldrich, USA), were used as received with purities of 99.8 and 99.5%, respectively. A measured mixture of TiO_2 and Li_2CO_3 (molar ratio Ti/Li of 2.27) were milled using a planetary ball mill (Retsch, PM100) for 2, 4, 6 and 8 hours with the addition of 10 wt.% PEG. The rotation of the ball mill was set in both directions. During the milling process, the interval time was set at 5 minutes with interval breaks at 10 seconds. Acetone solvent was used as a dispersing medium. The precursors were milled at 200 rpm with ball to powder ratio (BPR) of 10:1 at various milling time to form slurry. The slurry was dried at 80°C overnight to yield powder. The powder was pelletized and subsequently heat treated. The calcination process was carried out at 850°C for 12 h under N_2 atmosphere to produce spinel $Li_4Ti_5O_{12}$/C.

Thermal decomposition behaviour of the mixture of TiO_2-anatase and Li_2CO_3 was measured by thermo gravimetric analysis (TGA/DTA 6300, SII Nanotechnology Inc.) in flowing of N_2 atmosphere at temperature ranging from room temperature to 900°C with a heating rate of 5°C/min. The crystal structure of the powder samples were characterized by X-ray diffraction (XRD) using a Bruker AXS powder diffractometer, equipped with Cu $K_{\alpha1}$ radiation, $\lambda = 1.5406$ Å. XRD was operated at 40 kV and 30 mA, at scanning rate of 2°/min, between 10° and 80° of 2θ angle. The micrograph of the powder samples was examined by Field emission scanning electron microscopy (FESEM), using Leo 1525 electron microscope.

The electrochemical properties of the powder were evaluated using WonATech Battery Cycler System (WBCS 3000). The coin cells type CR 2032 was assembled with $Li_4Ti_5O_{12}$/C as anode and Li foil as reference electrode. The anode was prepared from a mixture of 0.02 g $Li_4Ti_5O_{12}$/C and 0.003g acetylene black with KFL 9305 as a binder. The mixture was pasted on stainless steel current collector grid and dried overnight. The electrolyte solution used was 1.0 M LiPF6 in a mixture of ethylene carbonate and dimethyl carbonate (EC: DMC) with ratio of 1:1. Microporous polypropylene sheet was used as the cell separator. The cell assembly was performed in a glove box (MBraun) filled with Ar gas. The charge-discharge cycling test was performed within the voltage region of 1.0 - 3.0 V vs. Li/Li$^+$ at room temperature. All electrochemical measurements were carried out at room temperature.
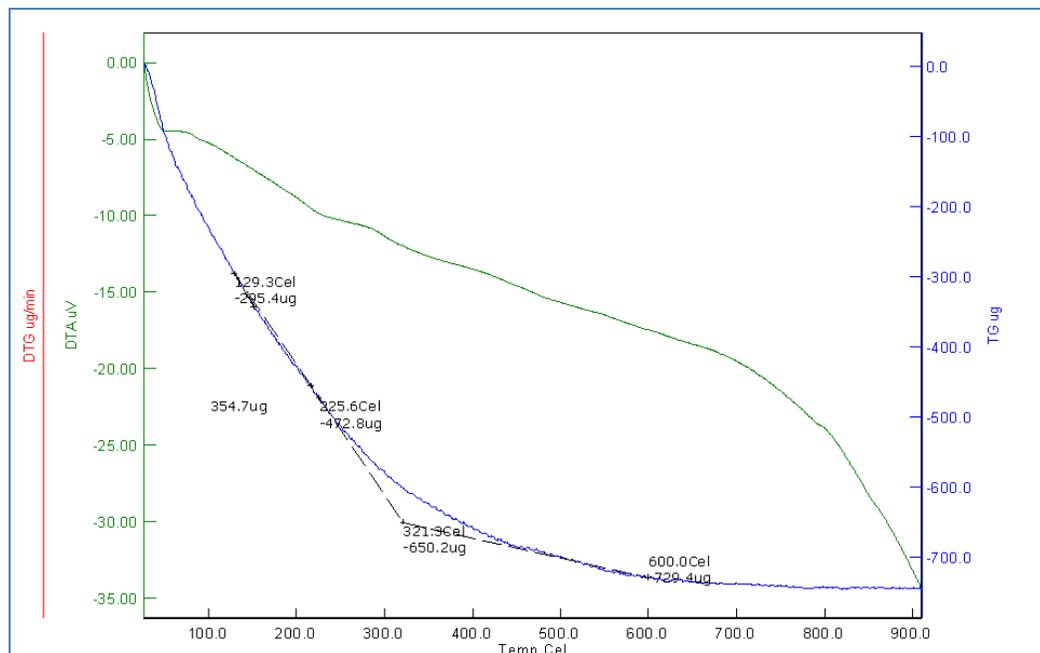
RESULTS AND DISCUSSION

Figure 1: TG/DTA results for $Li_4Ti_5O_{12}/C$

Figure 1 shows the TG-DTA results for non calcined $Li_4Ti_5O_{12}/C$. Results show very linear steps of weight loss. The first weight loss up to 350^0C was attributed to the vaporization of water and organic matters. The primary formation of $Li_4Ti_5O_{12}/C$ is assumed to occur between 350-600°C. No more weight loss is observed after 800°C which indicates the stability of the $Li_4Ti_5O_{12}/C$ material formed. This result suggests that the appropriate temperature to produce a stable $Li_4Ti_5O_{12}/C$ is around 800°C and above.

The ball-milling assisted solid state reaction route can be simply divided into three steps: i) the ball-milling process to generate titanate; ii) the annealing process to fabricate the spinel $Li_4Ti_5O_{12}/C$; iii) the washing process to produce pores. Accordingly, XRD patterns of $Li_4Ti_5O_{12}/C$ prepared at different milling time are shown in Figure 2. All the peaks can be indexed to the spinel phase structure of pure $Li_4Ti_5O_{12}$ [11]. In general, the absence of the principal peak characteristic of TiO_2 localized at $2\theta = 24\text{-}25^0$ in the product indicates the complete conversion of TiO_2 in the solid-state reaction [1]. There is not much difference observed between the diffraction peaks for the samples prepared at different milling time.
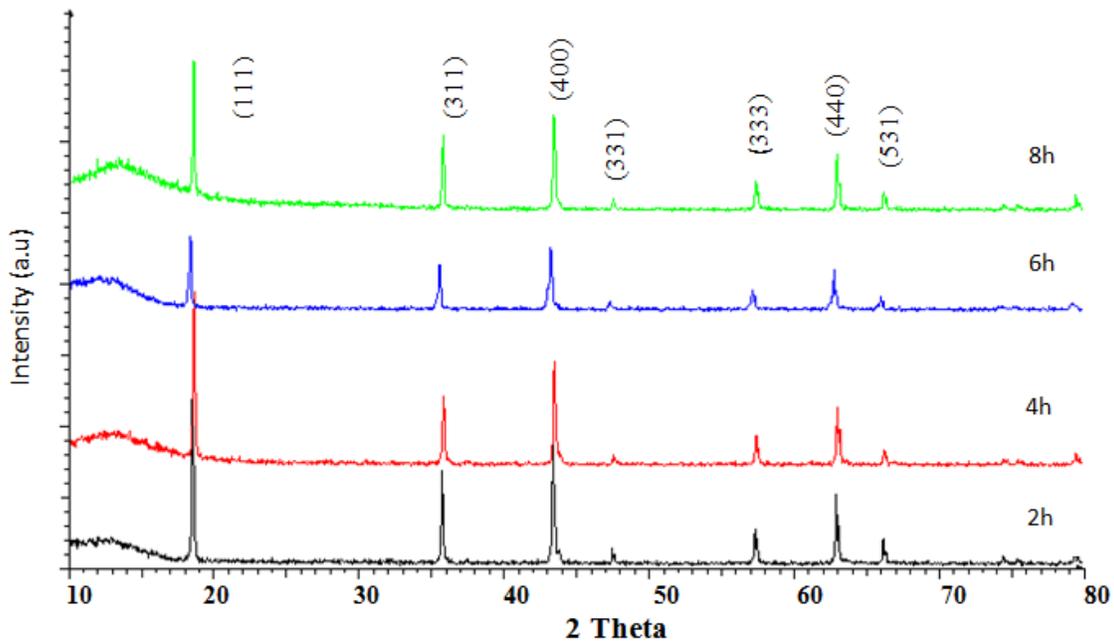
Figure 2: XRD results for $Li_4Ti_5O_{12}$/C milled at 2, 4, 6 and 8 hours and heated at 850°C

This indicates that a lower milling time of 2 hours is enough to fabricate pure $Li_4Ti_5O_{12}$. From the Joint Committee on Powder Diffraction Standards (JCPDS), the intensities were well reflected to the space group Fd3M. (111) peak further indicates that this material has a layered titanate structure. The lithium ions are located at the tetrahedral 8(a) sites, and tetravalent titanium ions (3d) and other lithium ions are randomly distributed at octahedral 16(d) sites by ratio Li/Ti = 1/5 while oxygen ions are located at the 32(e) sites. Therefore, this $Li_4Ti_5O_{12}$/C anode material can be suitably described as $Li_{4(8a)}[LiTi_5^{4+}]_{(16d)}O_{12(32e)}$ [12,13].
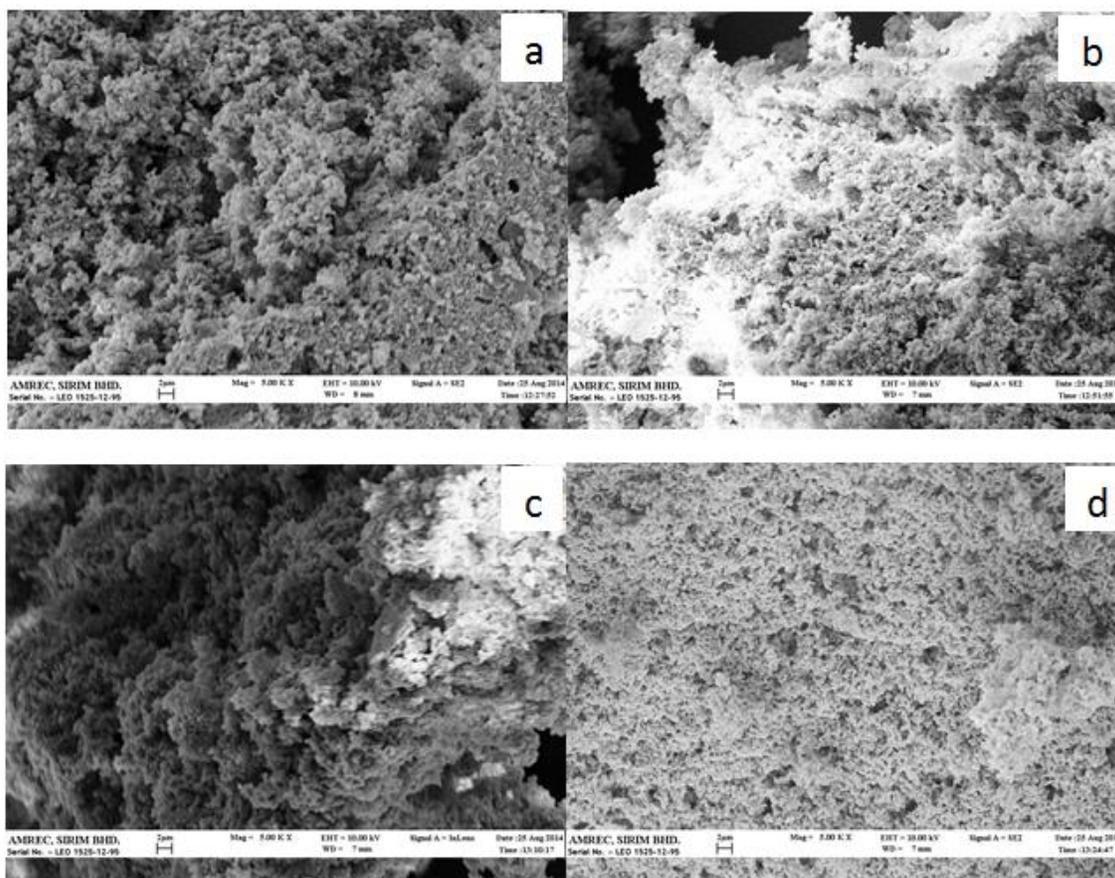
Figure 3: FESEM micrograph for $Li_4Ti_5O_{12}$/C ball milled at (a) 2 (b) 4 (c) 6 and 8 hours

FESEM analysis in Figure 3 shows the surface morphology of $Li_4Ti_5O_{12}$/C particles ball milled at different duration and heated at 850°C. Instead of just providing a carbon coating to increase conductivity, the purpose of using PEG, a gelatin agent with carboxylic (–COOH–) functional groups, also acts as a capping agent to prevent aggregation during synthesis[14]. However, some aggregation was observed in the FESEM images. It is well known that tailoring a particle morphology using the ball milling method is critical. Experiments conducted at different milling time can produce different particulate morphology. The average size of these samples as observed from the images in figure 3 are around 160-200 nm. FESEM micrograph in figure 3(a) showed a mixture of spherical and flaky shape due to shortened milling time. When milling time was increased, the microstructure of the samples exhibited a more homogenous spherical shape. Figure 3(d) revealed some agglomerations effects arising from a longer milling time of 8 hours.
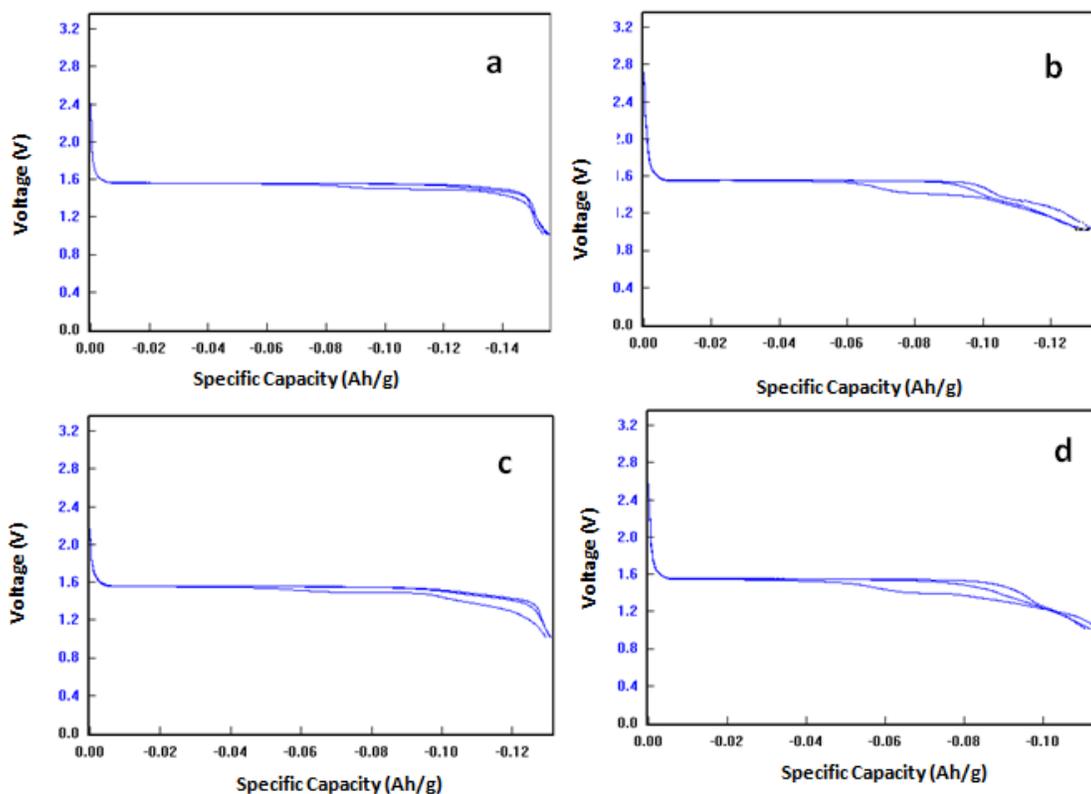
Figure 4: Discharge capacity of $Li_4Ti_5O_{12}/C$ ball milling for (a) 2, (b) 4, (c) 6 and (d) 8 hours

Figure 4 shows the 3 cycles of discharge profiles for samples ball milled at different duration. The cells were cycled between 1.0-3.0 V. The flat voltage plateau at around 1.55 V is associated with the two-phase lithium insertion and extraction processes of $Li_4Ti_5O_{12}/C$, indicating the well-developed crystalline phase of the $Li_4Ti_5O_{12}/C$ sample.

The capacities presented in this report are calculated based on the weight of active mass $Li_4Ti_5O_{12}/C$ powders. The stable plateau at 1.55 V vs. Li/Li^+, which originate from the intercalation/deintercalation of Li^+ ions on $Li_4Ti_5O_{12}/C$ framework is clearly visible for all of the samples. From the profiles, it was found that the specific discharge capacity of $Li_4Ti_5O_{12}/C$ decreases with increasing milling time. The discharge capacity values for 1st to 3rd cycles are (155, 154, 153), (132, 130, 129), (131, 131, 129) and (114, 111, 110) mAh/g for samples ball milled at 2, 4, 6 and 8h, respectively. The trend with lower discharge capacity obtained with longer milling time may be due to the pore structure breakdown which reduces Li^+ insertion process. $Li_4Ti_5O_{12}/C$ with 2 hours milling exhibits the highest initial discharge capacity (Li^+ insertion) of 155 mAh/g, indicating that a larger active material area is involved in the electrochemical reaction. For every sample, there is some irreversible capacity loss observed during the first cycle of the charge/discharge processes. This irreversible capacity loss may result from some non-

intercalation processes, such as electrode forming or corrosion of the current collector with solid electrolyte interface (SEI) formation [12].

The decline of specific discharge capacity with the milling time is attributed to the influence of particulate morphology of the synthesized $Li_4Ti_5O_{12}$/C. Wang et al. [15] who have studied the effect of milling time from 0-2 h by high energy ball milling (HEBM) on the formation of $Li_4Ti_5O_{12}$/C reported that the capacity reached the optimum value of 146.9 mAh/g at 1 h of milling time and the capacity decreased beyond this duration.

CONCLUSION

Single phase anode material of $Li_4Ti_5O_{12}$/C was successfully synthesized using ball milling assisted solid state reaction. The produced anode material has a spinel structure with high crystalline phase. The FESEM analysis showed that the agglomerated structure of $Li_4Ti_5O_{12}$/C powders has an average size of about 160-200 nm. The highest specific capacity is obtained from $Li_4Ti_5O_{12}$/C ball milled for 2 hours at 155 mAh/g when discharged at 10 mAg^{-1}. The specific discharge capacity decreases as the milling time is increased. The $Li_4Ti_5O_{12}$/C ball milled at 2 hours produces the best electrochemical performance as anode material.

ACKNOWLEDGEMENT

REFERENCES

[1]. A. Guerfi, P. Charest, K. Kinoshita,b, M. Perrier, K. Zaghib, *J. Power Sources* **126** 163-168 (2004)
[2]. T. Ohzuku, A. Ueda, N. Yamamoto, *J. Electrochem. Soc.* **142** 1431 (1995)
[3]. L. Zhao, Y.S. Hu, H. Li, Z.X. Wang, L.Q. *Chen, Adv. Mater.* **23** 1385 (2011)
[4]. J.Z. Chen, L. Yang, S.H. Fang, S. Hirano, K. Tachibana, *J. Power Sources* **200** 59 (2012)
[5]. Y.S. Lin, J.G. Duh, *J. Power Sources* **196** 10698 (2011)
[6]. K. Amine, I. Belharouak, Z.H. Chen, T. Tran, H. Yumoto, N. Ota, S.T. Myung, Y.K. Sun, *Adv. Mater.* **22** 3052 (2010)
[7]. J. Lu, C.Y. Nan, Q. Peng, Y.D. Li, *J. Power Sources* **202** 246 (2012)
[8]. S.L. Chou, J.Z. Wang, H.K. Liu, S.X. Dou, *J. Phys. Chem. C* **115** 16220 (2011)
[9]. H.G. Jung, S.T. Myung, C.S. Yoon, S.B. Son, K.H. Oh, K. Amine, B. Scrosati, Y.K. Sun, *Energy Environ. Sci.* **4** 1345 (2011)
[10]. K.M. Colbow, J.R. Dahn, R.R. Haering, *J. Power Sources* **26** 397 (1989)

[11]. C. Lai, Z. Z. Wu, Y. X. Zhu, Q. D. Wu, L. Li, C. Wang. *J. Power Sources* **226** 71-74 (2013)

[12]. M. Michalska, M. Krajewski, D. Ziolkowskac, B. Hamankiewicz, M. Andrzejczuk, L. Lipinska, K. P. Korona, A. Czerwinski, *J. Powder Technology* **266** 372-377 (2014)

[13]. K. Zaghib, M. Simoneau, M. Armand, M. Gauthier, *Journal of Power Sources* **81-82** 300-305 (1999)

[14]. V. Aravindan, K. Karthikeyan, K. S. Kang, W. S. Yoon, W. S. Kim, Y. S. Lee. *J. Materials Chemistry* **21** 2470-2475 (2011)

[15]. J. X. G. Wang, M. Wen, R. Cai, R. Ran, Z. Shao. *J. Solid State Ionics* **179** 946-950 (2008)